processes

MDPI

Article

Mass-Integration and Environmental Evaluation of Chitosan Microbeads Production Modified with of Thiourea and Magnetite Nanoparticles

Ángel Darío González-Delgado *, Grisel Cogollo-Cárcamo and Forlin Bertel-Pérez

Chemical Engineering Department, Nanomaterials and Computer Aided Process Engineering Research Group (NIPAC), Universidad de Cartagena, Cartagena 130014, Colombia;
gcogolloc@unicartagena.edu.co (G.C.-C.); fbertelp@unicartagena.edu.co (F.B.-P.)
* Correspondence: agonzalezd1@unicartagena.edu.co

Abstract: Bioadsorbents based on biopolymers modified with magnetic nanoparticles stand out for being non-toxic, effective, and easy to recover. Thus, the objective of the present work was to carry out a computer-aided environmental evaluation of the industrial-scale production of bioadsorbents from chitosan modified with iron nanoparticles and functionalized with thiourea as a chelating agent plus mass integration. The plant simulation was carried out in Aspen Plus, and for the mass integration of the process, a pinch analysis was used to determine the minimum target fresh and residual water amount, assuming two process stages: (1) the synthesis of magnetite nanoparticles, and (2) the production of chitosan-based bioadsorbents. The environmental assessment was performed using the waste reduction algorithm (WAR). The potential environmental impact (PEI) was quantified, taking into account the impact of the products and energy, obtaining a value below zero of −0.78 PEI/kg of the product. The photochemical oxidation potential (PCOP) stood out as the category with the greatest impact, mainly related to the use of ethanol during washing. The categories related to toxicological impacts (HTPI, HTPE, TTP, and ATP) had lower values than those related to atmospheric impacts (GWP, ODP, PCOP, and AP). The mass integration of the process resulted in fewer impacts in the HTPE category, as a consequence of the decrease in NaOH in the residual streams and the release of 0.297 PEI/kg of product in the ATP category caused by the presence of $Al(OH)_3$. It can be concluded that the mass integration managed to reduce up to 51% of the freshwater used in the processes, and it is a useful tool, as it slightly decreased the total potential impacts.

Keywords: bioadsorbents; environmental impact; mass integration; residual shrimp husk

Citation: González-Delgado, Á.D.; Cogollo-Cárcamo, G.; Bertel-Pérez, F. Mass-Integration and Environmental Evaluation of Chitosan Microbeads Production Modified with of Thiourea and Magnetite Nanoparticles. *Processes* **2023**, *11*, 2208. https://doi.org/10.3390/pr11072208

Academic Editors: Antoni Sanchez, Theodoros Karakasidis and Evangelos Karvelas

Received: 20 June 2023
Revised: 13 July 2023
Accepted: 21 July 2023
Published: 22 July 2023

1. Introduction

Chitosan is a linear N-acetyl polysaccharide derived from chitin. It is the second most abundant biopolymer in nature and can be produced from the exoskeletons of crustaceans such as shrimp, prawns, and lobsters, among others [1]. Chitosan finds extensive applications in agriculture [2,3], food [4,5], cosmetics, and pharmaceuticals [6], due to its hydrophilic nature [7], biocompatibility [6], biodegradability [8], antibacterial properties [9], remarkable affinity for biomacromolecules [10], and non-toxicity [11]. Moreover, it can be chemically modified to enhance its physical and chemical properties [12]. With its amino functional groups (-NH_2), chitosan has been widely used as an adsorbent for water treatment, removing dyes, organic pollutants, and heavy metals [13].

The increasing pollution of water bodies has driven the development of bioadsorbents with an enhanced mechanical strength, adsorption capacity, selectivity, and easy recovery. One of the modifying agents used to improve the recovery of chitosan-based bioadsorbents from treated waters is magnetite nanoparticles (Fe_3O_4), owing to their mixed-valence ferromagnetic nature with divalent and trivalent cations [14]. When particles are

scaled down to the nanometer range, they become superparamagnetic, preventing self-aggregation [15]. The modification of biopolymers, such as chitosan, lignin, cellulose, and poly-and (γ-glutamic acid), among others, with magnetite nanoparticles has been studied for the adsorption of contaminants such as methylene blue, eriochrome black T, and heavy metals. Specifically, magnetically modified chitosan offers advantages such as a strong metal chelation capacity due to the presence of amino and hydroxyl groups in the chitosan chain [16].

Likewise, the modification of biopolymers such as chitosan and alginate with thiourea improves the adsorption capacity of the biopolymers by increasing the number of active sites. This is because the thiol group forms stable complexes with metals such as Hg, Pt, Ag, Au, and to a lesser extent, Cd and Zn [17]. Thiourea-crosslinked chitosan microbeads exhibited an enhanced adsorption capacity for platinum due to their increased number of amino groups compared to unmodified chitosan, going from 80.6 mg/g to 129.9 mg/g using modified and unmodified chitosan, respectively [17]. Additionally, chitosan–magnetite nanocomposites have been successfully applied in the adsorption of toxic metals such as Pb(II) and Ni(II), and the beads were easily recovered through the application of a magnetic field [18].

Despite all the advantages of thiourea- and magnetically functionalized chitosan adsorbents, their production involves the use of a large amount of water, making it necessary to evaluate the use of optimization methodologies in this process. Thus, the design of an industrial-scale process using mass integration techniques can reduce the generation of wastewater and the consumption of freshwater [19,20]. Mass integration provides a holistic approach to the design, modernization, and operation of processes that emphasizes the unity of the process itself [21]. By considering the interaction between process units, resources, flows, and objectives, process integration enables a fundamental understanding of the overall knowledge of the process, systematically determines achievable performance targets, and facilitates systematic decision making to achieve these targets [22]. Recently, mass integration was implemented to minimize freshwater consumption in a yeast company through the optimization of the water utilization network using pinch methodology. This allowed for the recycling of 173,480.4 t/year of water within the system, demonstrating that 27% of freshwater usage can be saved [23].

Different bioadsorbent production processes have been evaluated from an environmental perspective using the Waste Reduction Algorithm (WAR), which takes into account the Potential Environmental Impacts (PEI) associated with chemical processes [24]. The evaluation of magnetite nanoparticle production using the co-precipitation method and the WAR algorithm revealed that the process does not generate significant negative impacts that could affect the ecosystem. It transforms feed streams with a high PEI into final products with a lower PEI, leading to the conclusion that large-scale magnetite production is environmentally applicable and respectful [25]. Regarding the synthesis of titanium dioxide, magnetite, and/or thiourea-modified chitosan microbeads, it was found that the presence of monovalent alcohols, such as ethanol (used in washing stages) and propanol (formed as an undesired product during hydrolysis in nanoparticle formation), increases the environmental effects related to the Photochemical Oxidation Potential (PCOP) category. However, overall, the process showed a moderately good performance [26].

This work aims to assess the environmental evaluation of the industrial-scale production of bioadsorbents from chitosan modified with iron nanoparticles and functionalized with thiourea as a chelating agent (BMCMN) combined with mass integration, using computer-aided engineering tools. This approach shows, for the first time, the use of computer-assisted process engineering (CAPE) strategies and the mass integration of processes to enhance the technical performance of a production topology for thiourea-modified chitosan bioadsorbents with magnetite, as well as the quantification of their generated environmental impacts, both upstream and under atmospheric and toxicological categories.

2. Materials and Methods

The methodology applied in this study consisted of the following stages: (i) mass integration, (ii) the process simulation of the integrated case, and (iii) an environmental evaluation using the Waste Reduction Algorithm (WAR). These stages were carried out to assess the proposal for the industrial production of bioadsorbents modified with chelating agents and magnetic nanoparticles (BMCMN). To develop the second stage, the Aspen Plus® software was used.

2.1. Process Production Modeling

Initially, the block diagram was designed based on the production process of BMCMN and the simulations were based on experimental data and previous information published by the research group [27]. For the scaling of the project, the availability of the raw materials was taken into account, resulting in a design of a plant with a processing capacity of 1746.2 tons of chitosan per year [28]. Objective flows were established, taking into account the experimentally reported flows that served as a basis for the process simulation. The block diagram for the designed topology is shown in Figure 1.

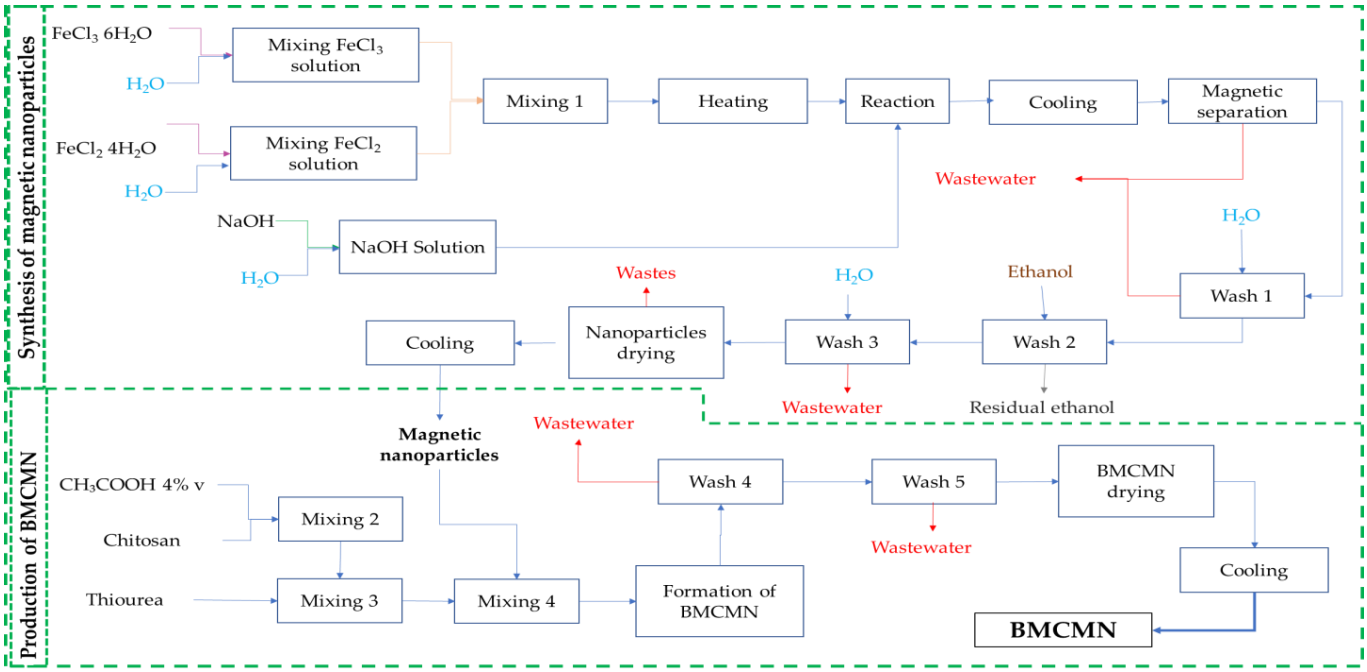

Figure 1. Block diagram of the production of BMCMN.

For the synthesis of magnetic nanoparticles using the co-precipitation method of $FeCl_3 \cdot 6H_2O$ and $FeCl_2 \cdot 4H_2O$, which were initially fed into the process in a molar ratio of 2:1 [29], they were fed with mass flow rates of 219.298 kg/h and 79.169 kg/h, respectively, and diluted in 4642.51 kg/h of water. The resulting solutions were mixed together via mechanical stirring (MIX-1), then heated to 80 °C [30], and sent to the reaction vessel, where 3505.58 kg/h of a 3M NaOH solution was added, raising the pH of the medium to approximately 12, allowing for the formation and precipitation of magnetic nanoparticles with a 98% conversion rate [31]. The resulting slurry was cooled to 28 °C and sent to magnetic separation, where 725.915 kg/h of nanoparticles were collected and separated from 7722.65 kg/h of the resting solution (wastewater). They were washed in three stages with 21,777.81 kg/h of water (wash 1) and 1842.89 kg/h of ethanol (wash 2 and 3) [31], and then dried in an oven at 105 °C and 1 bar [32]. It has been reported that the magnetic nanoparticles obtained using this method have a size distribution in the range of 10–500 nm, with a high purity [33].

For the synthesis of BMCMN, 180.71 kg/h of chitosan was initially dissolved in 9071.79 kg/h of a solution of acetic acid at 28 °C and 1 bar of pressure (Mixing 2). Subsequently, the solubilized chitosan was mixed with 90.36 kg/h of thiourea (Mixing 3), and the resulting stream (functionalized chitosan) was mixed with the synthesized magnetic nanoparticles (Mixing 4) for the formation of BMCMN under the same standard conditions (28 °C and 1 bar). The synthesized bioadsorbent was washed with water twice (wash 4 and 5), then dried at 105 °C to remove the excess of water, and cooled to 28 °C for storage.

For the study, the process was divided into two categories, as shown in Table 1:

Table 1. Process categories division of the production of BMCMN.

Category	Stage	Description
1	Synthesis of magnetic nanoparticles	The process begins by mixing $FeCl_3 \cdot 6H_2O$ and $FeCl_2 \cdot 4H_2O$ solutions and heating them to 80 °C. Then, the heated solutions are then combined with NaOH in a reactor to form magnetite, as shown in Equation (1). The resulting nanoparticles undergo purification before being utilized in the production of microbeads. To purify the nanoparticles, a magnetic separator is employed to separate the magnetite using an external magnetic field. The separated magnetite is subsequently washed and dried. $2FeCl_3 \cdot 6H_2O + FeCl_2 \cdot 4H_2O + 8NaOH \rightarrow Fe_3O_4 + 20H_2O + 8NaCl$ (1)
2	Production of the modified chitosan bioadsorbents	The chitosan is dissolved in an acetic acid solution to create a gel consistency. The substances to be impregnated are added to the gel, and the gel mixture is then dripped into a sodium hydroxide solution. This dripping process induces a liquid phase separation between acetic acid and NaOH, resulting in the formation of beads [34]. Subsequently, the beads go through a washing system where they are brought to a neutral pH, and finally, they are dried to reduce their water content

2.2. Simulation Procedure

The production of BMCMN was simulated using the commercial package Aspen Plus v12 (Bedford, MAX, USA), since the processes involve substances in the solid, liquid, and gas states; further, it has shown satisfactory results in the modeling and simulation of these type of processes, capturing the behavior [35,36]. The requirements for the consumables, utilities, and energy needs were calculated for the production of 1746.2 tons of chitosan per year. To accomplish this, the substances involved in the processes were initially selected from the simulator's chemical database. Subsequently, the thermodynamic model was chosen based on the algorithm described by Carlson [37]. Considering the aforementioned, the process conditions, and the chemical substances involved, a selection of appropriate models for predicting the thermodynamic properties was recommended. Among these models, ELECNRTL, a modified version of the Non-Random Two Liquids (NRTL) model for electrolytes, was suggested. This choice was motivated by the presence of both weak electrolytes, such as acetic acid, and strong electrolytes, such as NaOH and NaCl, in the system. Next, the conditions of the streams, including their mass, pressure, and temperature, were inputted. The necessary equipment for the different stages of the processes was selected, and the results were verified to ensure consistency with experimental data.

2.3. Mass Integration of Water Streams

Mass integration refers to a systematic methodology that provides a fundamental understanding of the overall mass flow within a process, enabling the identification of performance targets and the optimization of species generation and routing throughout the process [22]. A pinch analysis for water is a convenient tool for determining the minimum amount of water to be used, considering the recirculation of wastewater streams back into the process. In essence, this analysis takes into account the water requirements, both in terms of quantity and quality, for each process in the system. Quality is represented by

the concentration of critical contaminants in the stream and the contaminant load that can enter each stage [38]. These values can be established using algebraic approximations [39].

In the pinch analysis methodology, two important terms are used: the streams of residual water that can be utilized for reuse in the process are referred to as "sources", and the processes that can receive the reused water are known as "sinks". Firstly, the sinks were organized in ascending order based on their maximum allowable composition. Then, the sources were organized in ascending order according to their contaminant composition. The loads of the sinks and sources were calculated, taking into account Equations (2) and (3).

$$\dot{m}_j^{\sin k,\max} = G_j z_j^{\max} \tag{2}$$

$$\dot{m}_j^{source,\max} = w_i y_i \tag{3}$$

Subsequently, the accumulated loads were calculated by summing the individual loads of the sinks and sources, for each interval k, as shown in Equations (4)–(6). The accumulated loads were organized in ascending order, and load-interval diagrams (LID) were developed. Cascade diagrams were constructed, and residual streams were calculated for each interval. The most negative residual was set as the minimum target for freshwater consumption. Finally, the cascade diagram was reviewed, adding the maximum residual to the first interval and setting the residual interval to zero as the critical point for material recycling. The minimum waste discharge objective was determined as the residual at the outlet of the last interval [39].

For each interval k, the load and flow rates of the sources and sinks were calculated using Equations (4)–(6), respectively [21].

$$\Delta M_k = M_k - M_{k-1} \tag{4}$$

$$\Delta W_k = \frac{\Delta M_k}{y_{\text{source in interval k}}} \tag{5}$$

$$\Delta G_k = \frac{\Delta M_k}{z^{\max}_{\text{sink in interval k}}} \tag{6}$$

where ΔM_k is the interval load, ΔW_k is the source flow per interval, and ΔG_k is the sink flow per interval

On the other hand, the construction of the cascade diagrams was carried out using the data obtained from the LID. Figure 2a illustrates the flow balance for a given interval k, and the compilation of different intervals generated cascade diagrams, as shown in Figure 2b,c. The most negative value of the residual (δ_{max}) represents the objective for minimizing the consumption of freshwater to eliminate the existing infeasibilities. To achieve this, a fresh resource flow equal to δ_{max} was added at the input of interval 1 in the revised cascade diagram. The residual obtained in the last interval represents the objective for minimizing the generation of wastewater [39]. The described procedure provides the necessary information for the design of substance distribution networks.

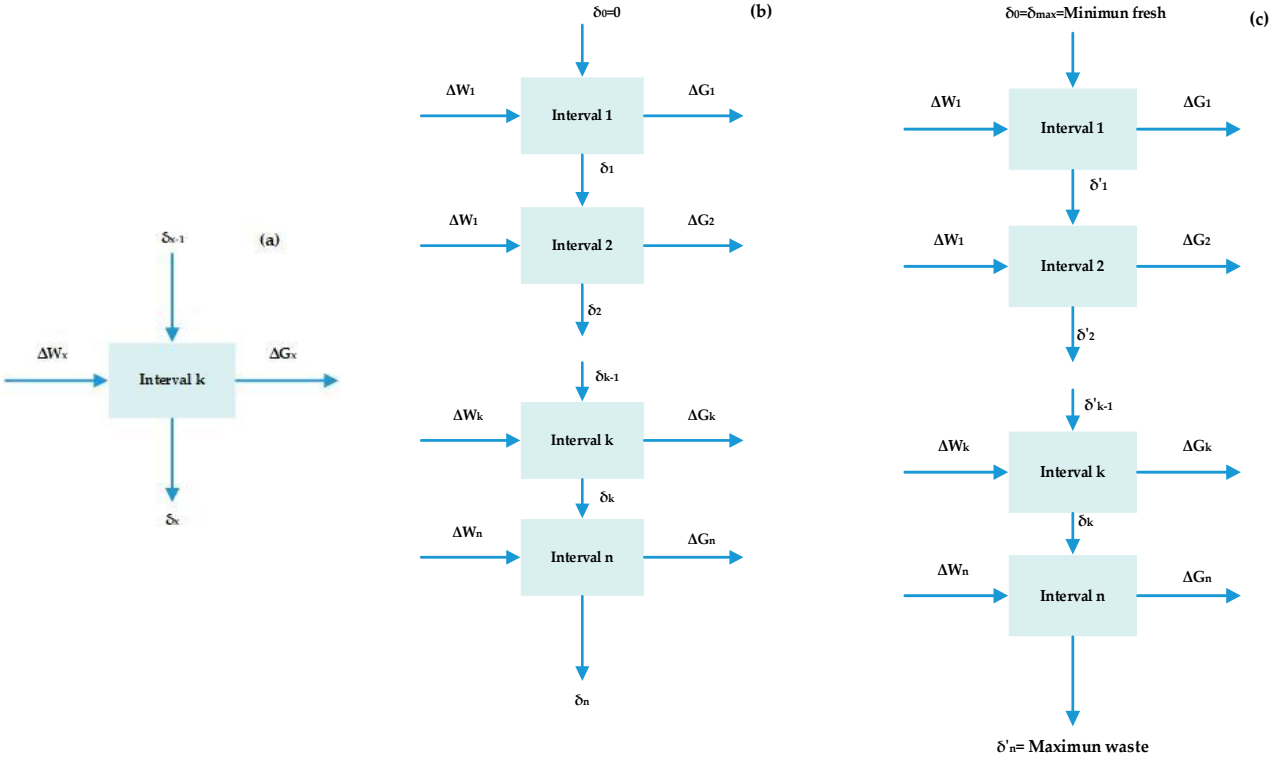

Figure 2. (**a**) Balance in interval k and cascade diagrams (**b**) initial and (**c**) revised. Adapted from El-Halwagi [39].

The mass integration of water streams in the synthesis process of BMCMN was carried out using the base case [40] as a starting point. The objective function was defined as the minimization of the freshwater requirements and wastewater effluents for the two stages considered in Section 2.1. Based on the flow and composition data obtained in the simulation, the sources and sinks to be considered for the integration were selected, taking into account the incoming freshwater streams and the residual streams predominantly composed of water. The critical contaminant in the effluents was identified and the addition of treatment units was established based on it. Subsequently, load-interval diagrams (LID) and cascade diagrams were generated, which were corrected if they had any negative residuals, allowing for the achievement of the minimum objectives for freshwater and wastewater. Finally, water distribution networks were designed for each studied subprocess, indicating which effluents should be recirculated to the different processes and in what quantity, to meet the minimum objectives established in the pinch analysis.

2.4. Environmental Assessment

The Waste Reduction Algorithm (WAR) (developed by the National Risk Management Research Laboratory of the U.S. Environmental Protection Agency) was used for the environmental impact assessment [41]. The potential environmental impact (PEI) of a given quantity of material and energy is a conservation relationship regarding the potential environmental impact based on the input and output impact flows of a process. The WAR–GUI software was used for calculating the PEI generated, considering eight environmental impact categories, four of which were related to atmospheric effects, while the remaining ones referred to toxicological effects. Within the atmospheric impact indices, there were two global categories: global warming potential (GWP) and ozone depletion potential (ODP), and two regional categories: photochemical oxidation potential (PCOP) and acidification potential (AP). On the other hand, the toxicological impact indices could be classified into human and ecological categories. The human indices included human toxicity potential by ingestion (HTPI) and that by inhalation or dermal exposure (HTPE),

while the ecological indices corresponded to aquatic toxicity potential (ATP) and terrestrial toxicity potential (TTP) [24]. In this work, Total Potential Environmental Impacts were used for the comparison of the processes, because they involved all the categories and were calculated by multiplying the mass flow rate by its chemical potential.

The first index, PEI_{OUT}, refers to the potential effects emitted to the environment external to the process and is useful for determining if a plant can produce a desired product while generating minimal environmental impact. The other index, PEIGEN, refers to the impacts generated by the system, and this indicator allows us to determine if the process was internally environmentally efficient. These PEIs can be calculated per unit of time using Equations (7) and (8).

$$i_{out}^{(t)} = i_{out}^{(cp)} + i_{out}^{(ep)} + i_{we}^{(cp)} + i_{we}^{(ep)} = \sum_{j}^{cp} \dot{M}_j^{(out)} \sum_{k} X_{kj}\Psi_k + \sum_{j}^{ep-g} \dot{M}_j^{(out)} \sum_{k} X_{kj}\Psi_k \quad (7)$$

$$i_{gen}^{(t)} = i_{out}^{(cp)} - i_{in}^{(cp)} + i_{out}^{(ep)} - i_{in}^{(ep)} + i_{we}^{(cp)} + i_{we}^{(ep)} = \sum_{j}^{cp} \dot{M}_j^{(out)} \sum_{k} X_{kj}\Psi_k - \sum_{j}^{cp} \dot{M}_j^{(in)} \sum_{k} X_{kj}\Psi_k + \sum_{j}^{ep-g} \dot{M}_j^{(out)} \sum_{k} X_{kj}\Psi_k \quad (8)$$

Additionally, the potential environmental impacts per unit mass of the products can be expressed using Equations (7) and (8).

$$\hat{i}_{out}^{(t)} = \frac{i_{out}^{(cp)} + i_{out}^{(ep)} + i_{we}^{(cp)} + i_{we}^{(ep)}}{\sum_P P_P} = \frac{\sum_j^{cp} \dot{M}_j^{(out)} \sum_k X_{kj}\Psi_k + \sum_j^{ep-g} \dot{M}_j^{(out)} \sum_k X_{kj}\Psi_k}{\sum_P P_P} \quad (9)$$

$$\hat{i}_{gen}^{(t)} = \frac{i_{out}^{(cp)} - i_{in}^{(cp)} + i_{out}^{(ep)} - i_{in}^{(ep)} + i_{we}^{(cp)} + i_{we}^{(ep)}}{\sum_P P_P} = \frac{\sum_j^{cp} \dot{M}_j^{(out)} \sum_k X_{kj}\Psi_k - \sum_j^{cp} \dot{M}_j^{(in)} \sum_k X_{kj}\Psi_k + \sum_j^{ep-g} \dot{M}_j^{(out)} \sum_k X_{kj}\Psi_k}{\sum_P P_P} \quad (10)$$

where $i_{in}^{(cp)}$ and $i_{out}^{(cp)}$ are the input rates of the PEI to the chemical process, $i_{in}^{(ep)}$ and $i_{out}^{(ep)}$ are the input and output rates of the PEI for the energy generation of the process, $i_{we}^{(cp)}$ and $i_{we}^{(ep)}$ are the PEIs related to the residual energy; $\dot{M}_j$ is the mass flow rate of the stream j, X_{kj} is the mass fraction of the component k in the stream j, and Ψ_k is the PEI of the k specie [24].

For the environmental assessment of the process, missing chemical species were initially added to the software database along with their environmental parameters. Then, the chemical species involved in the process that were already present in the database were selected. If they were not available, their CAS number, chemical formula, exact chemical formula, molecular weight, and toxicological data from the Material Safety Data Sheet (MSDS) were provided. With the simulation results from Aspen Plus, the compositions of each stream were identified, thus quantifying the generated waste and products. Once all the necessary information was provided to the software, the amounts of generated and emitted global potential impacts, both per unit mass and per unit time, for each category of the waste reduction algorithm, were obtained. The calculations also took into account the effect of the type of fuel on the environmental impacts of the processes, which were represented in bar graphs and data tables.

3. Results and Discussion

3.1. Mass-Integration

To perform the mass integration of the process, the algebraic approximation for the pinch analysis [42] was used to determine the minimum amount of fresh and residual water required. This analysis took into account both the quantity and quality of the water for reuse, with the latter being expressed in terms of the concentration of critical contaminants present [38]. In the evaluated topology, NaOH was identified as the critical contaminant, because one of the goals of the process washes was to achieve a pH close to neutral in the

product, and the presence of NaOH resulted in highly alkaline solutions. The maximum concentration limits of the critical contaminants in the inlet streams of the sinks were of great importance for the integration, as the tolerance to these contaminants would increase with their concentration. In this study, the maximum concentration of NaOH was selected, for which the solution pH still fell within the typical water quality requirements for the chemical industry, specifically, a maximum of 9 [43]. The division of the process into two stages (the synthesis of magnetite nanomaterial and the production of chitosan adsorbents functionalized with the chelating agent and nanomaterial) helped to protect the subprocesses, as once the integration was performed, the contaminants would only be present in each subprocess individually, and not in both at the same time.

The selection of the sinks used for the mass integration of the water streams in the process was carried out considering the limited information available regarding the influence of the contaminants in the water streams before the reactions and/or formation stages of the chitosan-modified bioadsorbents. This limitation restricted the number of sinks for evaluation, so only the water-washing stages (Wash 1, 3, 4, and 5) were taken into account, as summarized in Table 2. On the other hand, a total of five possible sources in the process located in the residual water streams from the magnetic separation and water washes were selected, as listed in Table 3.

Table 2. Selected sinks for mass integrations.

Category	Sink	$\dot{m}$ (kg/h)	X_{kj}	$\dot{I}_M$ (kg/h)	$\dot{I}_{MC}$ (kg/h)
1	Wash 1	21,777.43	4.04×10^{-7}	0.0088	0.0088
	Wash 3	7880.90	4.04×10^{-7}	0.0032	0.0120
2	Wash 5	135,535	4.04×10^{-7}	0.0547	0.0547
	Wash 4	90,356.47	4.04×10^{-7}	0.0365	0.0912

$\dot{I}_M$ is the maximum incoming impurity rate and $\dot{I}_{MC}$ is the maximum cumulative incoming impurity rate.

Table 3. Selected sources for mass integration.

Category	Sources	$\dot{m}$ (kg/h)	x_I	$\dot{I}$ (kg/h)	$\dot{I}_C$ (kg/h)
1	Wash 3 output	7582.49	1.45×10^{-6}	0.0110	0.0110
	Wash 1 output	21,173.17	3.17×10^{-5}	0.6715	0.6825
	Magnetic separator output	7544.91	1.14×10^{-3}	8.6315	9.3139
2	Wash 5 output	136,071.03	2.03×10^{-7}	0.0276	0.0276
	Wash 4 output	90,378.44	5.05×10^{-6}	0.4565	0.4841

x_I is the mass fraction of impurities, $\dot{I}$ is the impurity rate, and $\dot{I}_C$ is the cumulative incoming impurity rate.

Based on the information presented in Tables 1 and 2, it is evident that the quality of the residual water in terms of the NaOH concentration was considerably low for reuse in the selected sinks. Therefore, it was decided to treat the effluents to bring their pHs to acceptable levels. The selected treatment method involved adding aluminum sulfate to the alkaline water, resulting in the formation of solid aluminum and sodium sulfate. The solid aluminum was removed downstream of the reaction using filters, and the sodium sulfate posed no threat to the process. A 1% retention of the incoming liquid in the residual cake was considered [44]. It was determined that the output of Wash 5 met the required quality, and thus it was not treated. Once the sources were obtained within the parameters, as summarized in Table 4, the target quantities of the water consumption and waste generation were determined. From the data reported in Tables 2 and 4, load-interval diagrams (LIDs) and cascade diagrams were created for categories (1) and (2).

Table 4. Treated sources during the mass integration.

Category	Sources	$\dot{m}$ (kg/h)	x_I	$\dot{I}$ (kg/h)	$\dot{I}_C$ (kg/h)
1	Wash 3 output	7582.49	1.45×10^{-6}	1.09×10^{-6}	1.09×10^{-6}
	Wash 1 output	21,173.17	3.17×10^{-5}	6.65×10^{-5}	6.76×10^{-5}
	Magnetic separator output	7544.91	1.14×10^{-3}	8.55×10^{-4}	9.22×10^{-4}
2	Wash 5 output	136,071.03	2.03×10^{-7}	2.76×10^{-2}	2.76×10^{-2}
	Wash 4 output	90,378.44	5.05×10^{-6}	7.30×10^{-2}	1.01×10^{-1}

X_I is the mass fraction of impurities, $\dot{I}$ is the impurity rate, and $\dot{I}_C$ is the cumulative incoming impurity rate.

Figure 3 presents the LID obtained for the synthesis of the magnetite nanoparticles, while Figure 4 shows the corresponding cascade diagram for this subprocess. In this case, no negative residual was obtained, and therefore no correction was needed. It should be noted that the minimum requirement of freshwater for this process section was zero, and the minimum amount of residual water was approximately 6.3 t/h.

Interval	Load, kg/s 0.0	ΔM_k, kg/s	Sources	ΔW_k, kg/s	Sinks	ΔW_k, g/s
1	1.09×10^{-6}	0.0000	Source 1 $y = 1.45\times10^{-10}$	7,506.65		2.69
2	6.76×10^{-5}	0.0001	Source 2 $y = 3.17\times10^{-9}$	20,960.78	Sink 1 $z_{max}=4.04\times10^{-7}$	164.70
3	9.22×10^{-4}	0.0009	Source 3 $y = 1.15\times10^{-7}$	7,460.91		2117.06
4	8.79×10^{-3}	0.0079				19,492.98
5	1.20×10^{-2}	0.0032			Sink 2 $z_{max}=4.04\times10^{-7}$	7,880.90

Figure 3. LID for Magnetite Nanoparticle Synthesis (Category 1).

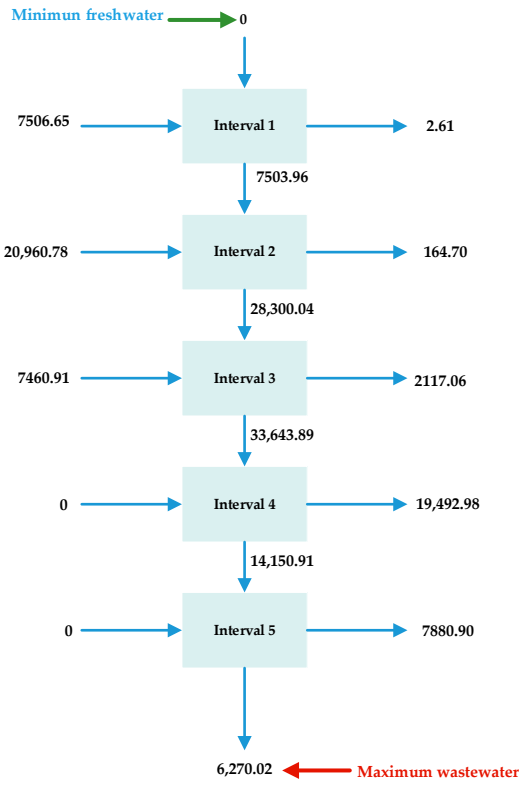

Figure 4. Cascade diagrams for Magnetite Nanoparticle Synthesis (Category 1).

On the other hand, Figures 5 and 6 show the load-interval diagram and cascade diagrams for the production of the chitosan microbeads, respectively. Upon reviewing the cascade diagram for this subprocess in Figure 6b, minimum targets of 11 t/h for freshwater and 7 t/h for residual water were established.

Interval	Load, kg/s	ΔM_k, kg/s	Sources	ΔW_k, kg/s	Sinks	ΔW_k, g/s
1	0.0276	0.0276	Source 1 $y = 2.03\times10^{-7}$	136,073.03		68,379.00
2	0.0547	0.0271		33,291.23	Sink 1 $z_{max}=4.04\times10^{-7}$	67,156.00
3	0.0912	0.0365	Source 2 $y = 8.14\times10^{-7}$	44,792.40	Sink 2 $z_{max}=4.04\times10^{-7}$	90,356.47
4	0.0094	0.0094		11,523.15		

Figure 5. LID for chitosan-based bioadsorbent (Category 2).

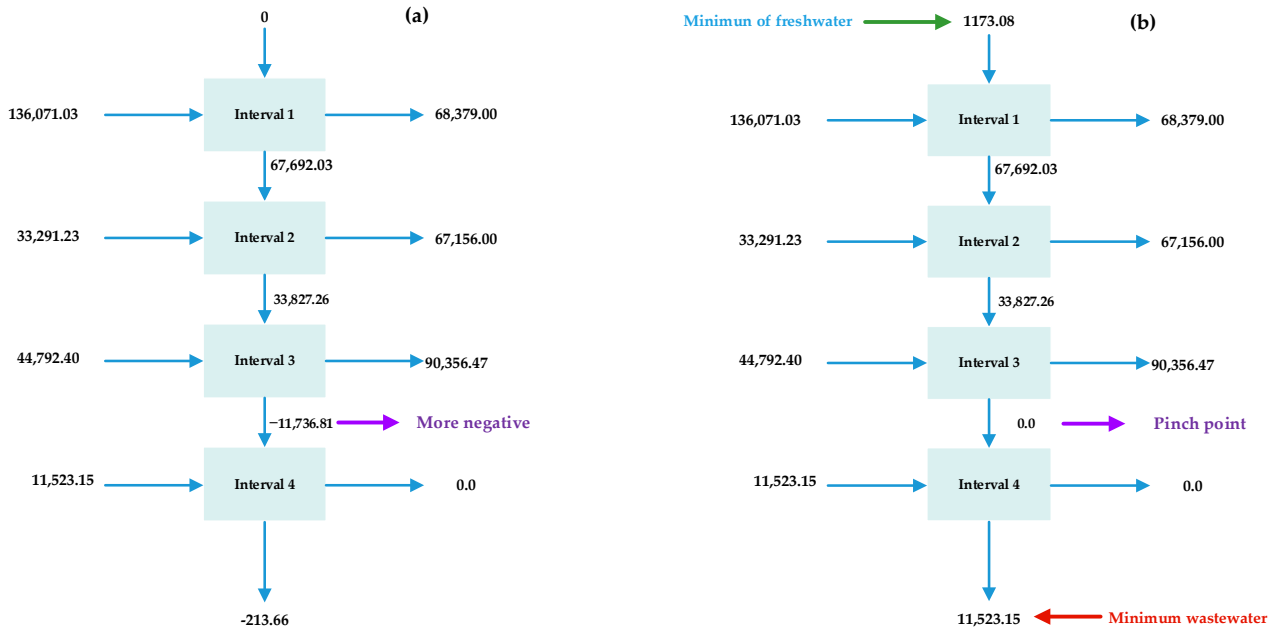

Figure 6. Cascade diagrams for Category 1 at (**a**) Base case and (**b**) mass-integrated topology.

It was determined that, for the selected sources and sinks in the base case, the minimum amount of freshwater that had to be fed to the washes was 11.7 t/h, and at least 17.8 t/h of wastewater would be discarded, with approximately 244 t/h being recirculated. Taking all of this into account, the water distribution network for topology I was designed, as illustrated in Figure 7. It can be observed that the quantities of freshwater and wastewater coincided with those obtained in the cascade diagrams.

3.2. Process Simulation

Figure 8 represents the simulation carried out for the integrated process of producing the chitosan adsorbents modified with thiourea and magnetite nanoparticles, when the blue streams are the integrated ones. The diagram shows the additional or manipulated streams in a blue color to achieve the mass integration of the system. For the simulation, only the treatment of the fractions of the residual streams that were to be recirculated was considered. Therefore, an ideal separator was placed in the residual stream of the magnetic separator to divide the flow to be utilized from the waste flow (F-1, F-2, and F-3). For simulation purposes, and considering that the algebraic integration only evaluated the presence of NaOH in the residual streams, 5% purges were implemented to control the amount of other contaminants that would be recirculated into the process and thus affect

the final product. The composition of the process streams leaving the units under study was sequentially cross-checked with the streams obtained in the non-integrated process. In cases where the overall concentration of different contaminants was very high, a higher purge was performed. This step was carried out through iterations.

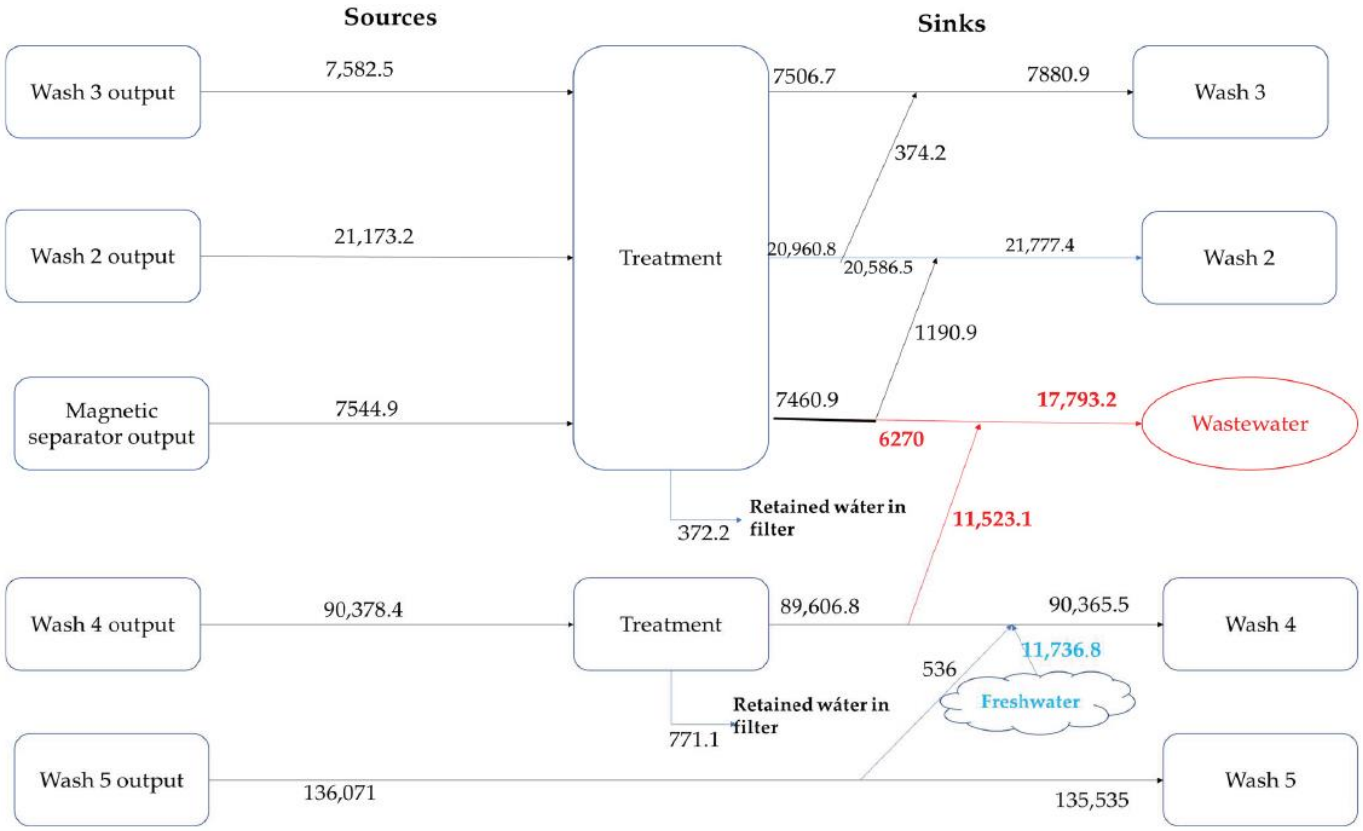

Figure 7. Water red distribution for the mass-integrated process.

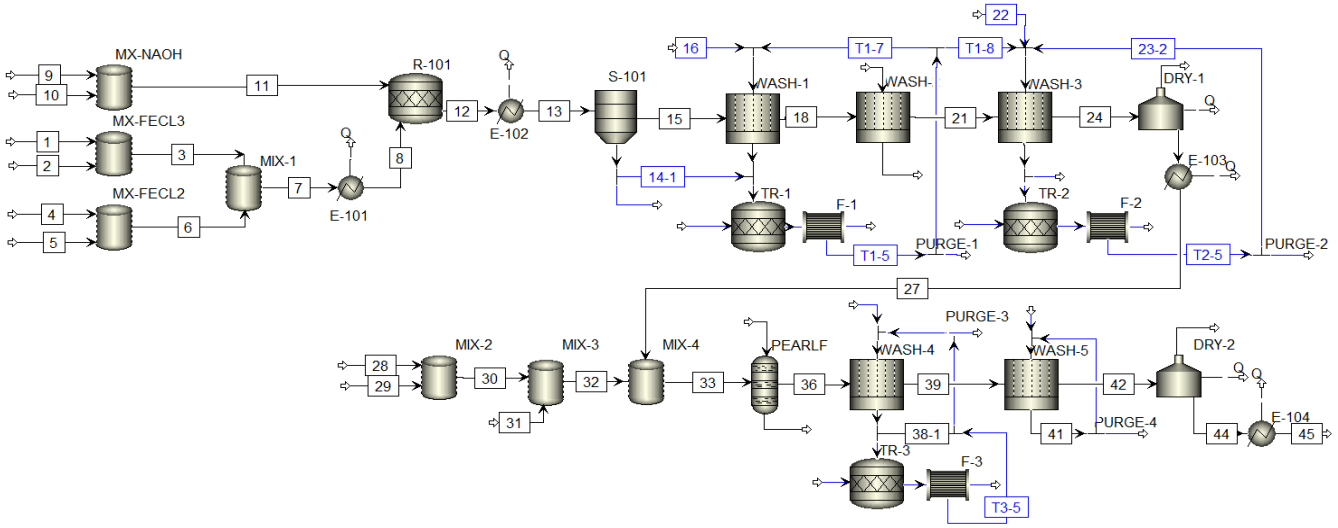

Figure 8. Simulation of the mass-integrated production process of BMCMN.

It was decided to locate three treatment sections in the plant: the first one to treat a fraction of the output stream from the magnetic separator, along with the output from washing step 1; the second one to treat a fraction of the output from washing step 3 due to the presence of ethanol in this stage, which needed to be controlled for safety reasons and

the amount of alcohol present in the nanoparticles; and the third one located at the output of washing step 4. Each treatment section was simulated by placing a reactor, in which the stoichiometric amount of alumina to be added was calculated, followed by a filter, where the liquid stream was separated from the solid aluminum hydroxide formed in the reactor.

The mass flows of the different raw materials and products of the process, intermediate and final, are found in Table 5.

Table 5. Main process streams obtained in the simulation for the production process of BMCMN.

Strem	**1**	**4**	**9**	**27**	**29**	**31**	**45**
Temperature (°C)	28	28	28	28	28	28	28
Pressure (bar)	1	1	1	1	1	1	1
Component mass flow (kg/h)							
Water	0.00	0.00	0.00	0.92	0.00	0.00	0.01
$FeCl_3 \cdot 6H_2O$	219.30	0,00	0.00	0.00	0.00	0.00	0.00
$FeCl_2 \cdot 4H_2O$	0.00	79.17	0.00	0.00	0.00	0.00	0.00
NaOH	0.00	0.00	134.21	0.00	0.00	0.00	0.00
Ethanol	0.00	0.00	0.00	0.01	0.00	0.00	0.00
Magnetite	0.00	0.00	0.00	90.36	0.00	0.00	52.49
NaCl	0.00	0.00	0.00	1.35	0.00	0.00	0.00
Acetic acid	0.00	0.00	0.00	0.00	0.00	0.00	0.00
Chitosan	0.00	0.00	0.00	0.00	180.71	0.00	104.98
Thiourea	0.00	0.00	0.00	0.00	0.00	90.36	52.49
$Al_2(SO_4)_3$	0.00	0.00	0.00	0.00	0.00	0.00	0.00
$Al(OH)_3$	0.00	0.00	0.00	0.00	0.00	0.00	0.00
$Na_2(SO_4)$	0.00	0.00	0.00	0.12	0.00	0.00	0.00
Total	219.30	79.17	134.21	92.77	180.71	90.36	209.97

Based on the results from Table 6, it can be stated that 130.6 t/h of water was successfully recirculated in the process, with more than one fifth corresponding to subprocess (2)—the synthesis of chitosan bioadsorbents, resulting in a 49.5% reduction in the total freshwater consumption and a 40.9% decrease in the residual water disposal. This was reflected in a total inventory reduction of up to 195.1 t/h in the integrated process.

Table 6. Quantities of fresh and residual water obtained in the simulation for the production of BMCMN.

Category	**Topology**	**FW_{MI} (kg/h)**	**FW_T (kg/h)**	**% FWR**	**WW_{IS} (kg/h)**	**WW_T (kg/h)**	**% WWR**
1	Base case	29,658.33	37,674.22	59.4%	36,291.25	37,228.38	60.7%
	Mass-integrated	7286.30	15,302.19		13,917.07	14,615.44	
2	Base case	225,891.47	225,891.47	47.9%	226,448.98	284,275.46	38.3%
	Mass-integrated	117,698.92	117,698.92		118,257.24	175,313.05	
Total	Base case	255,549.80	263,565.69	49.5%	262,740.23	321,503.84	40.9%
	Mass-integrated	124,985.22	133,001.11		132,174.31	189,928.49	

FW_{MI} is the freshwater for integrated streams, FWT is the total freshwater in the process, FWR is freshwater reduction, WW_{IS} is wastewater for integrated streams, WW_T is total wastewater, and WWR is wastewater reduction.

Additionally, Table 7 compares the reductions in water consumption in the process with the maximum possible according to the pinch analysis for the streams considered in the integration. The results show that the system could still be improved for both subprocesses (1) and (2), with the latter having greater opportunities for improvement than the former. However, this would require the addition of new treatments for the removal of other contaminants present in the wastewater, as they were limiting factors for the mass integration of the process.

Table 7. Reduction in freshwater and wastewater according to pinch analysis and real values.

Category	FW_{min} (kg/h)	% FWR_{Pinch}	FWR_{Real}	WW_{min} (kg/h)	% WWR_{Pinch}	% WWR_{Real}
1	0	100%	75.4%	6270.02	83%	61.7%
2	11,736.81	94.8%	47.9%	110,523.15	94.9%	47.8%
Total	11,736.81	95.4%	51.1%	17,793.17	93.2%	49.7%

FW_{min} is the minimum consumption of freshwater, FWR_{Pinch} is the freshwater reduction by pinch analysis, FWR_{Real} is the real freshwater reduction, WW_{min} is the minimum generation of freshwater, WWR_{Pinch} is wastewater reduction by pinch analysis, and WWR_{Real} is the real wastewater reduction.

A pinch analysis was used by Esmaeeli and Sarrafzadeh [45] for the Water Closed-Loop System (WCLS) in a pulp and paper (P&P) factory to reduce water consumption and wastewater. The water and steam network of the mill was synthesized, identifying the water sinks, sources, and flowrates, considering key pollutants (COD, TSS, and TDS), and the acceptable levels for the water sinks were established. A water pinch analysis with the direct-reuse approach was used to investigate each pollutant, achieving a maximum reduction in freshwater consumption of 36.9% by targeting TSS. The potential for reducing water consumption was lower for COD (4.0%) and TDS (18.9%). Khezri et al. [46] also applied water pinch technology to manage the industrial water consumption in the aluminum-anodizing industry, combining multiple index contaminants into a single contaminant. It was found that, by focusing on a key contaminant such as the total dissolved solids, the water usage was reduced by approximately 6.7%. Through the application of pinch technology and this new approach in three rinsing chambers, the water usage was further reduced by approximately 14.4%. These results were lower than those obtained in the present study per category, as shown in Table 7.

3.3. Environmental Assessment

The environmental assessment of the studied topology was carried out using the WARGUI software. However, the compounds $FeCl_3 \cdot 6H_2O$, $FeCl_2 \cdot 4H_2O$, chitosan, and magnetite were not available in the software's database, so it was necessary to consult the safety data sheets of the compounds to obtain the values for the different impact categories and add them to WARGUI. Once the compounds were added to the WARGUI database, the input and output streams, as well as the net heat flow of each process, were included. The results obtained for the evaluated topology are presented below. It is important to note that the reported data took into account the impact of the products and energy.

3.3.1. Total Environmental Impacts

The alternatives for bioadsorbent production were evaluated from an environmental perspective using the WAR methodology. Figure 9 shows the potential environmental impacts obtained for the studied topology.

A negative impact rate was obtained, reaching −0.78 PEI/kg of product for the topology and feed streams [47]. This could be attributed to the reaction that generated magnetite nanoparticles, as this material had considerably lower environmental impacts than the iron chlorides used as reactants. This difference was particularly notable in the HTPI, HTPE, and TTP impact categories. All of this confers a certain degree of environmental beneficence to the processes by reducing the potential impacts.

The values of the obtained output impacts reached magnitudes on the scale of thousands of PEI/h (ranging from 1871 to 2409 PEI/h), consistent with the data reported by Meramo et al. [26] for the production of TiO_2-modified chitosan microbeads. In that study, total impacts close to 4000 PEI/h were found to produce 2242 t/year of microbeads. In general, the magnetite-modified bioadsorbents exhibited a better environmental performance compared to those modified with TiO_2. This was because the TiO_2-modified bioadsorbents showed positive values of generated PEI, indicating that environmental impacts were

generated during the process, while in the case of the magnetite-modified beads, these impacts were reduced or eliminated.

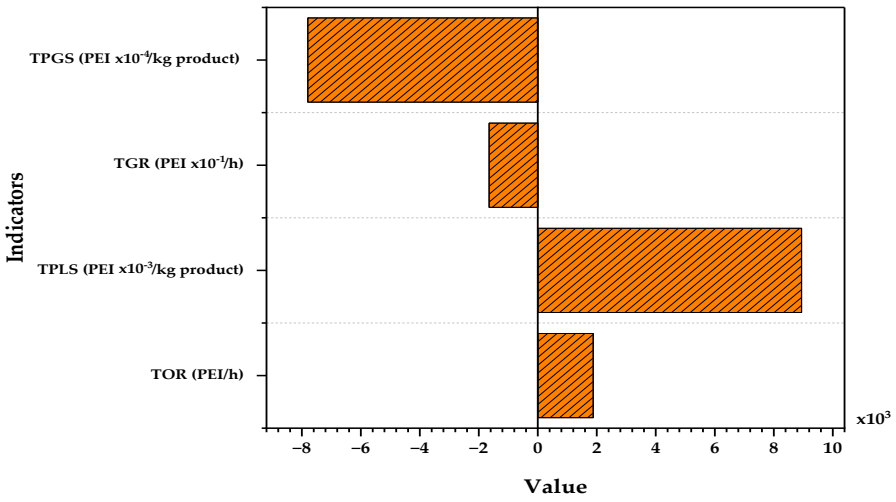

Figure 9. Total output and generated impacts per mass and time units, including the impact of the residues, the impact of the products, and the impact of the energy consumption.

Furthermore, it was observed that the difference in environmental performance when massively integrating the processes was minimal, with changes of less than 1% in the outgoing PEI and around 3% in the generated PEI compared to the base case [40]. This was because the recirculated species was water, which had no impact according to the WARGUI software. Therefore, the change in the environmental impacts of an integrated topology compared to the base case was related to the nature of the substances used in the effluent treatment to regulate their alkalinity. Specifically, higher total impacts were observed in the integrated cases due to the formation of aluminum hydroxide in the water treatment units, which affected the category of potential aquatic toxicity (ATP) and reduced the difference between the impacts at the inlet and outlet for this category.

In addition, the WAR algorithm has been successfully used for the environmental diagnosis of processes of different natures. In this regard, Petrescu and Cormos employed it in the environmental impact assessment of coal gasification with carbon capture and storage, finding that I_{out}, the total rate of the impact output, varied in the range of 70.86–134.85 PEI/MWh. This demonstrated that chemical looping cycles are very promising compared to gas–liquid absorption processes.

It was also used by de S. Lima et al. [48] for evaluating two process alternatives for a floating unit that aimed to capture and reuse CO_2 from natural gas. Alternative 1 involved combined dry and steam reforming in a single reactor, while Alternative 2 separated the reactions into two different reactors. Technical, economic, and environmental analyses were conducted using ASPEN HYSYS® and Capital Cost Estimation (CAPCOST) software. The potential environmental impacts were assessed using the Waste Reduction Algorithm (WAR) in terms of the PEI. The results indicated that Alternative 1 was the best option with a higher methanol production, lower CAPEX, higher sales revenue, and lower environmental impact index.

Further, two approaches were studied by Boltic et al. [49], and emissions versus the end of pipe (EOP) and cleaner production (CP) were analyzed to manage the pollution caused by tablet coating. The EOP approach focused on pollution control through process modification and the replacement of raw materials, considering cost-effectiveness and the pollution prevention criteria defined in the literature. The results from the implementation of the WAR methodology revealed that modifying the process design to prevent pollution in tablet coating provided significant benefits in terms of cost-effectiveness, waste/environmental impact reduction, and improved health and safety. Switching from organic solvents to

aqueous coating systems in the pharmaceutical industry is feasible with the availability of expertise, materials, and machines in the marketplace. The overall analysis of the WAR results supported the replacement of organic solvents with water in tablet coating. While liability and company image aspects were not included in this analysis, positive effects are expected in terms of public perception and compliance with environmental regulations.

3.3.2. Toxicological and Atmospheric Impacts

One of the advantages of the WAR methodology is that it allows for the evaluation and comparison of different process alternatives, even if they have different production capacities [50].

The contributions of each of the eight impact categories evaluated by the WARGUI software to the total environmental impact are presented in Figure 10. In all study cases, the photochemical oxidation potential (PCOP) stood out as the category with the highest impact, accounting for approximately 50% and 75% of the total output impacts for cases I and II, respectively. The results in Table 8 provide the scores assigned by the WARGUI software to each compound in the different impact categories. The PCOP impact was primarily related to the use of ethanol in wash 2, resulting in double the impact for the production of the microbeads modified solely with magnetite due to the double ethanol requirement, compared to the beads modified with thiourea and magnetite. In this regard, an alternative to reduce the impact in this category would involve replacing ethanol with another solvent with a lower environmental impact or reusing it in the second wash to reduce the need for fresh ethanol and the disposal of this compound.

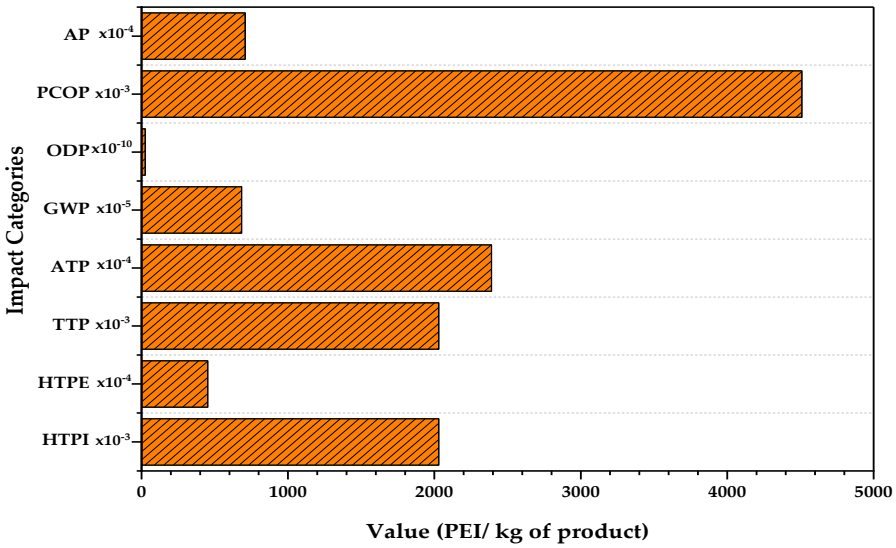

Figure 10. Output impacts by category considering the impact of the residues including the impact of the residues, the impact of the products and the impact of the energy consumption.

In general terms, the categories related to toxicological impacts (HTPI, HTPE, TTP, and ATP) presented lower values than the categories related to atmospheric impacts (GWP, ODP, PCOP, and AP). Among the former, it is worth highlighting the human toxicity by ingestion (HTPI) and potential terrestrial toxicity (TTP) categories, which were associated with the median lethal dose (LD_{50}) of the compounds involved in the process. The LD_{50} value was considerably low for thiourea, resulting in a higher environmental impact in these categories compared to the other substances involved in the process. This explains the greater contribution of these categories in the base case [40] compared to the mass-integrated case.

Table 8. Normalized environmental impact scores of compounds by impact category.

Compound	HTPI	HTPE	TTP	ATP	GWP	ODP	PCOP	AP
Water	0.000	0.000	0.000	0.000	0.000	0.000	0.000	0.000
$FeCl_2 \cdot 4H_2O$	0.202	0.239	0.202	0.005	0.000	0.000	0.000	0.000
$FeCl_3 \cdot 6H_2O$	0.382	0.034	0.382	0.000	0.000	0.000	0.000	0.000
NaOH	0.106	0.120	0.106	0.003	0.000	0.000	0.000	0.000
Ethanol	0.042	0.000	0.042	0.000	0.000	0.000	0.469	0.000
NaCl	0.125	0.000	0.125	0.000	0.000	0.000	0.000	0.000
Acetic acid	0.107	0.010	0.107	0.005	0.000	0.000	0.216	0.000
Chitosan	0.038	0.000	0.038	0.233	0.000	0.000	0.000	0.000
Thiourea	3.011	0.000	3.011	0.001	0.000	0.000	0.000	0.000
Magnetite	0.038	0.024	0.038	0.000	0.000	0.000	0.000	0.000
Na_2SO_4	0.107	0.000	0.107	0.000	0.000	0.000	0.000	0.000
$Al(OH)_3$	0.094	0.017	0.094	3.604	0.000	0.000	0.000	0.000
$Al_2(SO_4)_3$	0.195	0.018	0.195	0.012	0.000	0.000	0.000	0.000

Furthermore, it is worth noting that the mass-integrated case of the base scenario [40] had opposite effects on the total output impact, as observed in Figure 11. However, this was directly related to changes in the output impacts for the HTPE and ATP categories, which were attributed to the presence of aluminum sulfate in the input streams of the process as a reagent to treat the caustic soda present in the wastewater streams, as well as aluminum hydroxide and sodium sulfate in the residual streams from the washes. In this regard, the mass-integrated topology showed slightly lower impacts in the HTPE category due to the reduction in NaOH in the residual streams, and it generated an additional 0.03 PEI/kg of product in the ATP category compared to the base process, due to the presence of $Al(OH)_3$ in the mass-integrated case.

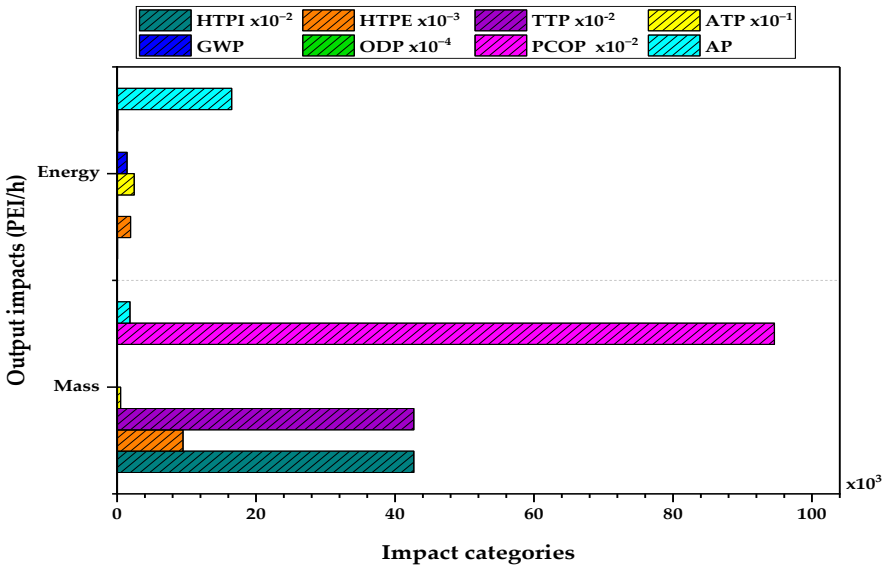

Figure 11. Contribution by mass and energy to the output PEI for the mass-integrated case, including the impact of the residues and the product and considering natural gas as energy source.

3.3.3. Contribution of Energy to Output Impacts

To consider the contribution of energy to the generated impacts, the WARGUI software offers three fuel options: natural gas, petroleum, and coal. In the current study cases, natural gas was chosen due to its lower environmental impact associated with energy consumption. However, the contribution of energy to the total impacts was generally not significant, both for the processes as a whole and for the individual categories, as shown in Figure 11. The

exceptions were the global warming potential (GWP), ozone depletion potential (ODP), and acidification potential (AP), which were fully determined by the contribution of energy.

In summary, since the base case and the mass-integrated scenario both generated negative impacts, this indicates that, overall, the processes did not create impacts, but rather consumed them [50]. The mass integration of the processes was favorable from an environmental perspective, as it slightly reduced the overall impacts. However, this was achieved at the expense of a lower economic profitability of the process due to the increased amount of equipment required [51].

4. Conclusions

The environmental assessment using the Waste Reduction Algorithm (WAR) for a mass-integrated approach to the industrial production of bioadsorbents modified with chelating agents and magnetic nanoparticles (BMCMN) was carried out to determine its Potential Environmental Impacts (PEI). From the simulation, it was found that the mass-integrated topology achieved a product flow of 2029.89 t/year, with a processing capacity of 5503.36 t/year. The application of mass integration through the design of water distribution networks based on a pinch analysis enabled a recirculation of 130.6 t/h, reducing the consumption of freshwater by 49.5. This allowed for a decrease of 40.9 in wastewater compared to the base case.

The processes evaluated in this research demonstrated a good environmental performance, as evidenced by the negative total generated impacts. The optimization of the process in terms of water usage did not have significant effects on the environmental and process safety indicators. From a toxicological and atmospheric perspective, it was found that the HTPI and TTP categories presented the highest PEI indices, which was attributed to the handling of substances such as $FeCl_2 \cdot 4H_2O$, $FeCl_3 \cdot 6H_2O$, and thiourea. In this regard, ethanol had effects on the atmospheric categories, with the PCOP category contributing approximately 70% to the environmental impacts from these sources. The process generated fewer environmental impacts than similar processes, such as the production of bioadsorbents modified with TiO_2 nanoparticles and magnetite-TiO_2 (1870 PEI/h vs. 4000 PEI/h vs. 4970 PEI/h, respectively). In terms of process safety, the associated indices remained constant or varied in a way that kept the index unchanged.

5. Future Approach

Considering the obtained results from the environmental analysis the plus mass integration assisted by the CAPE strategies, it would be advisable to evaluate the application of mass integration for substances other than water, aiming to utilize the materials lost during the washing stages. This would have a positive impact in environmental terms by reducing the Potential Environmental Impact (PEI) associated with the emission of these substances. For future studies, it is recommended to investigate different laboratory-scale water treatment methods to find the most suitable mechanism for this particular process, in order to reduce the impact of the massive integration of wastewater on the quality of the final product. This would also allow for a higher proportion of water to be recycled in the system. Additionally, it is suggested to consider replacing ethanol with a solvent in the second wash that generated lower impacts related to photochemical oxidation potential (PCOP). Since this category was predominant in the evaluated topology, substituting the alcohol would result in a significant reduction in the potential environmental impacts at the end of the processes. This approach would be accurate with the results obtained by Boltic et al. [49] for table coating processing in the pharmaceutical industry.

It would also be beneficial to use other methodologies for assessing and reducing environmental impacts, such as the Tool for Reduction and Assessment of Chemicals and Other Environmental Impacts (TRACI) or Life Cycle Assessment (LCA). Additionally, conducting a safety analysis using the Inherent Safety Index (ISI) would allow for the identification of process risks, which would reflect the social impacts of the process.

Author Contributions: Conceptualization, Á.D.G.-D.; methodology, Á.D.G.-D.; software, F.B.-P. and G.C.-C.; validation, Á.D.G.-D.; formal analysis, F.B.-P. and G.C.-C.; investigation, F.B.-P., G.C.-C. and Á.D.G.-D.; resources, Á.D.G.-D.; data curation F.B.-P. and G.C.-C.; writing—original draft preparation, F.B.-P. and G.C.-C.; writing—review and editing, Á.D.G.-D.; visualization, F.B.-P. and G.C.-C.; supervision, Á.D.G.-D.; project administration, Á.D.G.-D.; funding acquisition, Á.D.G.-D. All authors have read and agreed to the published version of the manuscript.

Funding: This research received no external funding.

Data Availability Statement: The data that support the findings of this study are available from the corresponding author, Á.D.G.-D., upon reasonable request.

Acknowledgments: The authors thank the Universidad de Cartagena to provide the software and required equipment to successfully conclude this research project.

Conflicts of Interest: The authors declare no conflict of interest.

References

1. Carballo, E.; Martínez, E. *Determinación de la Permeabilidad al Vapor de Agua Por el Método ASTM E96/E 96M-05 en Películas de Quitosano*; Universidad de El Salvador: San Salvador, El Salvador, 2010.
2. Kumaraswamy, R.V.; Kumari, S.; Choudhary, R.C.; Pal, A.; Raliya, R.; Biswas, P.; Saharan, V. Engineered chitosan based nanomaterials: Bioactivities, mechanisms and perspectives in plant protection and growth. *Int. J. Biol. Macromol.* **2018**, *113*, 494–506. [CrossRef]
3. El Hadrami, A.; Adam, L.R.; El Hadrami, I.; Daayf, F. Chitosan in Plant Protection. *Mar. Drugs* **2010**, *8*, 968–987. [CrossRef]
4. Irastorza, A.; Zarandona, I.; Andonegi, M.; Guerrero, P.; de la Caba, K. The versatility of collagen and chitosan: From food to biomedical applications. *Food Hydrocoll.* **2021**, *116*, 106633. [CrossRef]
5. Flórez, M.; Guerra-Rodríguez, E.; Cazón, P.; Vázquez, M. Chitosan for food packaging: Recent advances in active and intelligent films. *Food Hydrocoll.* **2021**, *124*, 107328. [CrossRef]
6. Martău, G.A.; Mihai, M.; Vodnar, D.C. The Use of Chitosan, Alginate, and Pectin in the Biomedical and Food Sector—Biocompatibility, Bioadhesiveness, and Biodegradability. *Polymers* **2019**, *11*, 1837. [CrossRef]
7. Cohen, E.; Poverenov, E. Hydrophilic Chitosan Derivatives: Synthesis and Applications. *Chem.—A Eur. J.* **2022**, *28*, e202202156. [CrossRef]
8. Lee, K.Y.; Ha, W.S.; Park, W.H. Blood compatibility and biodegradability of partially N-acylated chitosan derivatives. *Biomaterials* **1995**, *16*, 1211–1216. [CrossRef]
9. Li, J.; Tian, X.; Hua, T.; Fu, J.; Koo, M.; Chan, W.; Poon, T. Chitosan Natural Polymer Material for Improving Antibacterial Properties of Textiles. *ACS Appl. Bio Mater.* **2021**, *4*, 4014–4038. [CrossRef] [PubMed]
10. Yi, H.; Wu, L.Q.; Bentley, W.E.; Ghodssi, R.; Rubloff, G.W.; Culver, J.N.; Payne, G.F. Biofabrication with chitosan. *Biomacromolecules* **2005**, *6*, 2881–2894. [CrossRef]
11. Chen, Y.; Wang, J. Removal of radionuclide Sr2+ ions from aqueous solution using synthesized magnetic chitosan beads. *Nucl. Eng. Des.* **2012**, *242*, 445–451. [CrossRef]
12. Rinaudo, M. Chitin and chitosan: Properties and applications. *Prog. Polym. Sci.* **2006**, *31*, 603–632. [CrossRef]
13. Karimi, M.H.; Mahdavinia, G.R.; Massoumi, B.; Baghban, A.; Saraei, M. Ionically crosslinked magnetic chi-tosan/kappa-carrageenan bioadsorbents for removal of anionic eriochrome black-T. *Int. J. Biol. Macromol.* **2018**, *113*, 361–375. [CrossRef]
14. Mazo-zuluaga, J. Una mirada al estudio y las aplicaciones tecnológicas y biomédicas de la magnetita. *Rev. EIA* **2011**, *16*, 207–223.
15. Noval, V.E.; Puentes, C.O. Magnetita (Fe_3O_4): Una estructura inorgánica con múltiples aplicaciones en catálisis heterogénea. Rev. Colomb. *Química* **2016**, *46*, 42–59.
16. Lasheen, M.; El-Sherifb, I.Y.; Tawfik, M.E.; El-Wakeel, S.; El-Shahat, M. Preparation and adsorption properties of nano magnetite chitosan films for heavy metal ions from aqueous solution. *Mater. Res. Bull.* **2016**, *80*, 344–350. [CrossRef]
17. Zhou, L.; Liu, J.; Liu, Z. Adsorption of platinum(IV) and palladium(II) from aqueous solution by thiourea-modified chitosan microspheres. *J. Hazard. Mater.* **2009**, *172*, 439–446. [CrossRef]
18. Tran, H.V.; Dai Tran, L.; Nguyen, T.N. Preparation of chitosan/magnetite composite beads and their application for removal of Pb(II) and Ni(II) from aqueous solution. *Mater. Sci. Eng. C* **2010**, *30*, 304–310. [CrossRef]
19. Feng, X.; Huang, L.; Zhang, X.; Liu, Y. Water system integration of a brewhouse. *Energy Convers. Manag.* **2009**, *50*, 354–359. [CrossRef]
20. Morales, M. Aplicación de tecnología asistida por computadora para la integración eléctrica en trenes. *1er Congr. De Manuf. Av.* **2014**, *26*, 1–10.
21. El-Halwagi, M.M. *Pollution Prevention through Process Integration: Systematic Design Tools*; Academic Press: Cambridge, MA, USA, 1997.
22. El-Halwagi, M.M. *Process Integration*; Elsevier: Houston, TX, USA, 2006.
23. Xu, X.; Lv, Z.; Song, Y.; Bin, L. Water system integration and optimization in a yeast enterprise. *Resour. Conserv. Recycl.* **2015**, *101*, 96–104. [CrossRef]

24. Young, D.M.; Cabezas, H. Designing sustainable processes with simulation: The waste reduction (WAR) algorithm. *Comput. Chem. Eng.* **1999**, *23*, 1477–1491. [CrossRef]
25. Arteaga-Díaz, S.J.; Meramo-Hurtado, S.I.; León-Pulido, J.; Zuorro, A.; González-Delgado, A.D. Environmental Assessment of Large Scale Production of Magnetite (Fe_3O_4) Nanoparticles via Coprecipitation. *Appl. Sci.* **2019**, *9*, 1682. [CrossRef]
26. Meramo-Hurtado, S.; Urbina-Suaréz, N.; González-Delgado, Á. Computer-aided environmental and exergy analyses of a large-scale production of chitosan microbeads modified with TiO_2 nanoparticles. *J. Clean. Prod.* **2019**, *237*, 117804. [CrossRef]
27. Solano, R.A.; De León, L.D.; De Ávila, G.; Herrera, A.P. Polycyclic aromatic hydrocarbons (PAHs) adsorption from aqueous solution using chitosan beads modified with thiourea, TiO_2 and Fe_3O_4 nanoparticles. *Environ. Technol. Innov.* **2021**, *21*, 101378. [CrossRef]
28. Cogollo-Herrera, K.; Bonfante-Álvarez, H.; De Ávila-Montiel, G.; Barros, A.H.; González-Delgado, A.D. Techno-economic sensitivity analysis of large scale chitosan production process from shrimp shell wastes. *Chem. Eng. Trans.* **2018**, *70*, 2179–2184. [CrossRef]
29. Tao, K.; Dou, H.; Sun, K. Interfacial coprecipitation to prepare magnetite nanoparticles: Concentration and temperature dependence. *Colloids Surf. A Physicochem. Eng. Asp.* **2008**, *320*, 115–122. [CrossRef]
30. Alfaro, I.; Molina, L.; González, P.; Gaete, J.; Valenzuela, F.; Marco, J.; Sáez, C.; Basualto, C. Silica-coated magnetite nanoparticles functionalized with betaine and their use as an adsorbent for Mo(VI) and Re(VII) species from acidic aqueous solutions. *J. Ind. Eng. Chem.* **2019**, *78*, 271–283. [CrossRef]
31. Yazdani, F.; Edrissi, M. Effect of pressure on the size of magnetite nanoparticles in the coprecipitation synthesis. *Mater. Sci. Eng. B* **2010**, *171*, 86–89. [CrossRef]
32. Bui, T.Q.; Ton, S.N.-C.; Duong, A.T.; Tran, H.T. Size-dependent magnetic responsiveness of magnetite nanoparticles synthesised by co-precipitation and solvothermal methods. *J. Sci. Adv. Mater. Devices* **2018**, *3*, 107–112. [CrossRef]
33. Hadadian, Y.; Sampaio, D.R.; Ramos, A.P.; Carneiro, A.A.; Mozaffari, M.; Cabrelli, L.C.; Pavan, T.Z. Synthesis and characterization of zinc substituted magnetite nanoparticles and their application to magneto-motive ultrasound imaging. *J. Magn. Magn. Mater.* **2018**, *465*, 33–43. [CrossRef]
34. Vakili, M.T.; Rafatullah, M.; Ibrahim, M.H.; Abdullah, A.Z.; Salamatinia, B.; Ghoiami, Z. Preparation of Chitosan Beads for the Adsorption of Reactive Blue 4 from Aqueous Solutions. *Iran. J. Energy Environ.* **2016**, *7*, 124–128. [CrossRef]
35. García-Padilla, Á.; Moreno-Sader, K.A.; Realpe, Á.; Acevedo-Morantes, M.; Soares, J.B. Evaluation of adsorption capacities of nanocomposites prepared from bean starch and montmorillonite. *Sustain. Chem. Pharm.* **2020**, *17*, 100292. [CrossRef]
36. Zuorro, A.; Moreno-Sader, K.A.; González-Delgado, Á.D. Evaluating the feasibility of a pilot-scale shrimp biorefinery via techno-economic analysis. *J. Clean. Prod.* **2021**, *320*, 128740. [CrossRef]
37. Carlson, E.C. Don't Gamble with Physical Properties. *Chem. Eng. Prog.* **1996**, 35–46.
38. Brouckaert, C.; Buckley, C. *Water Pinch Analysis: A Strategic Tool for Water Management in the Food Processing Industry, University of Natal*; University of Natal: Durban, South Africa, 1997.
39. El-Halwagi, M.M. *Direct-Recycle Networks: An Algebraic Approach, in Sustainable Design through Process Integration*; Butterworth-Heinemann: Oxford, UK, 2012; pp. 223–229.
40. Bertel, F.; Cogollo, G.; Meramo-Hurtado, S.; González-Delgado, A. Computer aided environmental analysis of a large-scale production of chitosan micro-beads modified with thiourea and magnetite. *IOP Conf. Series: Mater. Sci. Eng.* **2019**, *519*, 012003. [CrossRef]
41. Obando, J.J.J. Evaluacion Tecno-Economica de la Produccion de Biocombustibles a Partit de Microalgas. Ph.D. Thesis, Universidad Nacional de Colombia, Bogotá, Colombia, 2011; p. 109.
42. El-Halwagi, M.M. *Sustainable Design through Process Integration: Fundamentals and Applications to Industrial Pollution Prevention, Resource Conservation, and Profitability Enhancement*; Butterworth-Heinemann: Waltham, MA, USA, 2012.
43. *CSIRO and Institute for Sustainability and Innovation Guidance for the Use of Recycled Water by Industry*; Smart Water Fund: Victoria, BC, Canada, 2008; Volume 174.
44. CETESB Capítulo 8: Tratamiento de agua. In *Operación y Mantenimiento de Plantas de Tratamiento de Agua: Manual de Capacitación para Operadores*; CEPIS (Ed.) CEPIS: Brussels, Belgium, 2002; Volume 862.
45. Esmaeeli, A.; Sarrafzadeh, M.-H. Reducing freshwater consumption in pulp and paper industries using pinch analysis and mathematical optimization. *J. Water Process. Eng.* **2023**, *53*, 103646. [CrossRef]
46. Khezri, S.M.; Lotfi, F.; Tabibian, S.; Erfani, Z. Application of water pinch technology for water and wastewater minimization in aluminum anodizing industries. *Int. J. Environ. Sci. Technol.* **2010**, *7*, 281–290. [CrossRef]
47. Arteaga-Díaz, S.; Sanjuan-Acosta, M.J.; González-Delgado, Á. Computer-aided environmental evaluation of bioethanol production from empty palm fruit bunches using oxalic acid pretreatment and molecular sieves. *Chem. Eng. Trans.* **2018**, *70*, 2113–2118. [CrossRef]
48. Lima, B.C.d.S.; de Araújo, O.Q.F.; de Medeiros, J.L.; Morgado, C.R. Technical, Economic and Environmental Viability of Offshore CO_2 Reuse from Natural Gas by Dry Reforming. *Appl. Mech. Mater.* **2016**, *830*, 109–116. [CrossRef]
49. Boltic, Z.; Ruzic, N.; Jovanovic, M.; Savic, M.; Jovanovic, J.; Petrovic, S. Cleaner production aspects of tablet coating process in pharmaceutical industry: Problem of VOCs emission. *J. Clean. Prod.* **2013**, *44*, 123–132. [CrossRef]

50. Moreno-Sader, K.; Meramo-Hurtado, S.; González-Delgado, A. Computer-aided environmental and exergy analysis as decision-making tools for selecting bio-oil feedstocks. *Renew. Sustain. Energy Rev.* **2019**, *112*, 42–57. [CrossRef]
51. Meramo-Hurtado, S. *Modelo de Optimización de Biorefinería Multifeedstock Considerando Parámetros Ambientales, Económicos y de Seguridad*; Universidad de Cartagena: Cartagena, Colombia, 2017.